THE JOURNAL OF BIOLOGICAL CHEMISTRY VOL. 284, NO. 22, pp. 14849–14856, May 29, 2009

Structural Evidence of Substrate Specificity in Mammalian Peroxidases

STRUCTURE OF THE THIOCYANATE COMPLEX WITH LACTOPEROXIDASE AND ITS INTERACTIONS AT 2.4 Å RESOLUTION[*S]

Received for publication, October 2, 2008, and in revised form, March 18, 2009 Published, JBC Papers in Press, April 1, 2009, DOI 10.1074/jbc.M807644200

Ishfaq Ahmed Sheikh[1], **Amit Kumar Singh**[2], **Nagendra Singh, Mau Sinha, S. Baskar Singh, Asha Bhushan, Punit Kaur, Alagiri Srinivasan, Sujata Sharma, and Tej P. Singh**[3]

From the Department of Biophysics, All India Institute of Medical Sciences, New Delhi 110 029, India

The crystal structure of the complex of lactoperoxidase (LPO) with its physiological substrate thiocyanate (SCN^-) has been determined at 2.4 Å resolution. It revealed that the SCN^- ion is bound to LPO in the distal heme cavity. The observed orientation of the SCN^- ion shows that the sulfur atom is closer to the heme iron than the nitrogen atom. The nitrogen atom of SCN^- forms a hydrogen bond with a water (Wat) molecule at position 6′. This water molecule is stabilized by two hydrogen bonds with Gln^{423} $N^{\epsilon 2}$ and Phe^{422} oxygen. In contrast, the placement of the SCN^- ion in the structure of myeloperoxidase (MPO) occurs with an opposite orientation, in which the nitrogen atom is closer to the heme iron than the sulfur atom. The site corresponding to the positions of Gln^{423}, Phe^{422} oxygen, and $Wat^{6'}$ in LPO is occupied primarily by the side chain of Phe^{407} in MPO due to an entirely different conformation of the loop corresponding to the segment Arg^{418}–Phe^{431} of LPO. This arrangement in MPO does not favor a similar orientation of the SCN^- ion. The orientation of the catalytic product $OSCN^-$ as reported in the structure of LPO·$OSCN^-$ is similar to the orientation of SCN^- in the structure of LPO·SCN^-. Similarly, in the structure of LPO·SCN^-·CN^-, in which CN^- binds at Wat^1, the position and orientation of the SCN^- ion are also identical to that observed in the structure of LPO·SCN.

Lactoperoxidase (LPO[4]; EC 1.11.1.7) is a Fe^{3+} heme enzyme that belongs to the mammalian peroxidase family (1). The family of mammalian peroxidases comprises lactoperoxidase (2), eosinophil peroxidase (3), thyroid peroxidase (4), and myeloperoxidase (MPO) (5). LPO, eosinophil peroxidase, and MPO are responsible for antimicrobial function and innate immune responses (6–8), whereas thyroid peroxidase plays a key role in thyroid hormone biosynthesis (9). These peroxidases are different from plant and fungal peroxidases because unlike plant and fungal enzymes, the prosthetic heme group in mammalian peroxidases is covalently linked to the protein (10). There are also several striking structural and functional differences among the mammalian peroxidases (11). The heme group in MPO is attached to the protein via three covalent linkages (12), whereas LPO (12, 13), eosinophil peroxidase (12), and thyroid peroxidase (12) contain only two ester linkages. These covalent and various non-covalent linkages contribute differentially to the high stability of the heme core as well as for the peculiar values of their redox potentials (2, 14). Furthermore, MPO consists of two disulfide-linked protein chains, whereas LPO, eosinophil peroxidase, and thyroid peroxidase are single chain proteins, although their chain lengths differ greatly. In addition, their sequences contain several critical amino acid differences that may also contribute to the variations in the stereochemical environments of the substrate-binding sites. As a consequence of these differences, the mammalian enzymes oxidize various inorganic ions such as SCN^-, Br^-, Cl^-, and I^- with differing specificities and potencies. Biochemical studies have shown that LPO catalyzes preferentially the conversion of SCN^- to $OSCN^-$ (15, 16), whereas MPO uses halides (17, 18) with a preference for chloride ion as the substrate. The preferences of eosinophil peroxidase and thyroid peroxidase are bromide and iodide, respectively. However, the stereochemical basis of the reported preferences for the substrates by mammalian heme peroxidases is still unclear. So far, the structures of only two mammalian enzymes, MPO and LPO, have been determined (12, 13). It is of considerable importance to identify the structural parameters that are responsible for the subtle specificities. In the present work, we have attempted to address this question through the new crystal structures of LPO complexes with SCN^- ions using goat, bovine, and buffalo lactoperoxidases. Because the overall structures of complexes of SCN^- with LPO from all three species were found to be identical, the structure of the complex of buffalo LPO with SCN^- and the ternary complex with SCN^- and CN^- will be discussed here, and buffalo LPO will be termed hereafter as LPO. To highlight the factors pertaining to binding

* This work was supported in part by the Department of Science and Technology, New Delhi.

[S] The on-line version of this article (available at http://www.jbc.org) contains supplemental data, Figs. S1–S3, and Refs. 1–3.

The atomic coordinates and structure factors (codes 3FAQ, 3ERI and 3ERH) have been deposited in the Protein Data Bank, Research Collaboratory for Structural Bioinformatics, Rutgers University, New Brunswick, NJ (http://www.rcsb.org/).

[1] Supported by a fellowship from the University Grants Commission, New Delhi.

[2] Supported by a fellowship from the Council of Scientific and Industrial Research, New Delhi.

[3] Distinguished Biotechnologist of the Department of Biotechnology, New Delhi. To whom correspondence should be addressed: Dept. of Biophysics, All India Institute of Medical Sciences, Ansari Nagar, New Delhi 110 029, India. Tel.: 91-11-2658-8931; Fax: 91-11-2658-8663; E-mail: tpsingh.aiims@gmail.com.

[4] The abbreviations used are: LPO, lactoperoxidase; MPO, myeloperoxidase; Wat, water; ABTS, 2,2-azinobis(3-ethylbenzthiazolinesulfonic acid).

specificity of SCN^-, a comparison of the structures of LPO·SCN^- and MPO·SCN^- has also been made, revealing many valuable differences pertaining to the observed orientations of the common substrate, SCN^- ion, when bound at the substrate-binding site in the distal heme cavity of the two structures. The structures of LPO·SCN^- and MPO·SCN^- clearly show that the bound SCN^- ions are present in the distal heme cavity of two enzymes with opposite orientations. In the structure of LPO·SCN^-, the sulfur atom is closer to the heme iron than the nitrogen atom, whereas in that of MPO·SCN^-, the nitrogen atom is closer to the heme iron than the sulfur atom. As a result of this, the interactions of the SCN^- ion in the distal site of two proteins differ drastically. Gln^{423}, a conserved water (Wat) molecule at position 6′, and a well aligned carbonyl oxygen of Phe^{422} in the proximity of the substrate-binding site in LPO against a protruding Phe^{407} in MPO seem to play the key roles in inducing the observed orientations of SCN^- ions in LPO and MPO. The structure of LPO·SCN^- has also been compared with the structure of its ternary complex with SCN^- and CN^- ions.

EXPERIMENTAL PROCEDURES

Purification of the Protein—Lactoperoxidase-catalyzed oxidation of SCN^- in milk and saliva contributes to the antimicrobial activity of these fluids (19). Lactoperoxidase was isolated from milk samples collected from Murrah buffaloes (*Bubalus bubalis*) available at the Indian Veterinary Research Institute (Izatnagar, India). The fat was separated from the fresh milk by skimming. Buffer containing 50 mM Tris-HCl, pH 8.0, and 2 mM $CaCl_2$ was added to the skimmed milk. The cation exchanger CM-Sephadex C-50 (7 g $liter^{-1}$) (GE Healthcare, Uppsala, Sweden) equilibrated in 50 mM Tris-HCl, pH 7.8, was added and stirred slowly with a glass rod for ~1 h. The gel was kept overnight undisturbed at 280 K. It was decanted on the next day. The unbound proteins were removed by washing the gel with an excess of 50 mM Tris-HCl, pH 8.0. The washed gel was loaded on a CM-Sephadex C-50 column (10 × 2.5 cm) and equilibrated with 50 mM Tris-HCl, pH 8.0. The protein samples were eluted using a linear gradient of 0.0–0.5 M NaCl with the same buffer. The protein fractions eluted at 0.2 M NaCl were pooled, desalted, and concentrated using an Amicon ultrafiltration cell. This was loaded on a Sephadex G-100 column (100 × 2 cm) using 50 mM Tris-HCl buffer, pH 8.0. This was eluted using the same buffer at a flow rate of 6.0 ml/h. The various protein fractions were collected and pooled separately. These protein samples were examined on SDS-PAGE. The fractions corresponding to an approximate molecular mass of 68 kDa were pooled, lyophilized, and stored at −20 °C for further analysis. The N-terminal sequence of the first 20 amino acid residues was also determined using Edman degradation with Protein Sequencer PPSQ-21A (Shimadzu, Japan).

LPO Activity Measurements—The activity assay was carried out following the procedure of Shindler and Bardsley (20) with some modifications to suit certain requirements. 3.0 ml of 1 mM 2,2-azinobis(3-ethylbenzthiazolinesulfonic acid) (ABTS) in 0.1 M phosphate buffer, pH 6.0, was mixed with 0.1 ml of sample in 0.1 M phosphate buffer, pH 7.0, containing 0.1% gelatin to initialize the spectrophotometer (PerkinElmer Life Sciences). 3.0 ml of 1 mM ABTS solution was mixed with 0.1 ml of protein sample and 0.1 ml of 3.2 mM hydrogen peroxide solution. The absorbance was measured at 412 nm as a function of time for 2 to 3 min. The rate of change of absorbance was constant for at least 2 min. 1 unit of activity is defined as the amount of enzyme catalyzing the oxidation of 1 μmol of ABTS min^{-1} at 293 K (molar absorption coefficient 32,400 M^{-1} cm^{-1}). The activity of lactoperoxidase was found to be 5.3 units ml^{-1}. The purity of LPO was also determined by absorbance ratio A_{412}/A_{280} (*RZ* value). The *RZ* value for the purified LPO was found to be 0.932. In addition to this, two separate binding experiments were also carried out using buffers containing 50% methanol as the first condition and using 3 M NaCl as the second condition.

Crystallization of LPO and Its Complexes—The purified samples of LPO were dissolved in 0.01 M phosphate buffer, pH 6.0, containing 2 mM $CaCl_2$ to a concentration of 25 mg/ml. A reservoir solution consisting of 0.2 M ammonium iodide and 20% (w/v) polyethylene glycol 3350 was prepared. 3 μl of protein solution was mixed with 3 μl of reservoir solution to prepare 6 μl of drops for hanging drop vapor diffusion method. The rectangular dark brown-colored crystals of LPO measuring up to $0.3 \times 0.3 \times 0.2$ mm^3 were obtained after 1 week. The crystals of the complex of LPO with SCN^- were prepared by soaking the crystals of native LPO in the mother liquor composed of 20% (w/v) polyethylene glycol 3350, 0.01 M sodium phosphate, 2 mM $CaCl_2$, 50 mM NaSCN at 24 °C at pH 6.0 for 48 h. The crystals of the complex of LPO with the SCN^- ion were soaked in the mother liquor containing 20% (w/v) polyethylene glycol 3350, 0.01 M sodium phosphate, 2 mM $CaCl_2$, 50 mM sodium cyanate (NaCN) at 25 °C at pH 6.0 for 48 h.

Detection of SCN^- Ions in Crystals—To confirm the presence of the SCN^- ion in the soaked crystals of LPO, the crystals were washed thoroughly with distilled water. The washed crystals were crushed. This solution was incubated with 1 M NaCl for 1 h and then ultrafiltered using a membrane with a molecular mass cutoff of 1 kDa. The presence of SCN^- ions in the filtrate was detected by colorimetric determination of SCN^- ions in the sample (21). To make ferric thiocyanate, the ferric nitrate reagent was prepared by dissolving 1 g of ferric nitrate crystals in 10 ml of Milli-Q water, to which 10 ml of concentrated nitric acid was added for making the final volume to 200 ml. 2 ml of the filtrate was mixed with equal volume of the ferric nitrate reagent. The resulting appearance of red color confirms the presence of SCN^- ions in the crystal filtrate.

Spectroscopic Analysis of LPO·SCN^- Crystal—The spectral changes in the heme absorption at 412 nm were also recorded spectrophotometrically (PerkinElmer Life Sciences spectrophotometer). To determine the presence of SCN^- ions in the crystals, three different solutions were made. Solution 1 contained the dissolved protein crystals. Solution 2 was obtained after removing the small molecular contents from solution 1 after incubating it with 1 M NaCl and ultrafiltrating it using a membrane with a molecular mass cutoff of 1 kDa. Solution 3 was prepared by mixing purified protein and potassium thiocyanate. The absorption spectra were recorded on all the three samples using a wavelength of 412 nm.

X-ray Intensity Data Collection—The x-ray intensity data were collected at 285 K using a 345-mm diameter MAR

Research dtb imaging plate scanner mounted on a Rigaku RU-300 rotating anode x-ray generator operating at 100 mA and 50 kV. The CuK_{α} radiation was obtained using Osmic Blue confocal optics. The intensities were processed using programs DENZO and SCALEPACK (22). The space group was found to be monoclinic $P2_1$ with approximate cell dimensions of $a = 54.2$, $b = 80.5$, and $c = 77.3$ Å and $\beta = 102.7°$. The final data set shows an overall completeness of 98.6% for resolution to 2.4 Å. The summary of final data collection statistics are given in Table 1.

Structure Determination and Refinement—The crystal structures of LPO·SCN^- (bovine), LPO·SCN^- (buffalo) and LPO·SCN^-·CN^- (buffalo) were determined with molecular replacement method using the principle of maximum likelihood in PHASER (23). The native structure of LPO (Protein Data Bank Code 2R5L) was used as the search model (13). The rotation and translation search functions were computed using reflections in the resolution range of 12.0–4.0 Å. This yielded clear solutions with distinct peaks in each case. The molecular packing in the unit cell calculated using coordinates from these solutions did not produce unfavorable short contacts. The coordinates were transferred using PHASER (23) and were subjected to 25 cycles of rigid body refinement with REFMAC (24) from the CCP4i Version 4.2 program package (25). After the first rounds of refinement, the R_{work} and R_{free} factors reduced to the range between 0.30 and 0.33 and between 0.40 and 0.41, respectively. (5% of the reflections were used for the calculation of R_{free}; the reflections were not included in the refinement.) The initial maps showed good electron densities for the heme groups. The coordinates of the heme groups were included in further rounds of refinement that were carried out with intermittent manual model building of the protein using Fourier $|2F_o - F_c|$ and difference Fourier $|F_o - F_c|$ maps with graphics program O (26) and Coot (27) on a Silicon Graphics O_2 workstation. In the refinement calculations, the ligand-Fe restraints were not used. At the end of these refinements, the R_{work} and R_{free} factors converged to ~0.248 and 0.278, respectively, for the structures of LPO·SCN^- (bovine), LPO·SCN^- (buffalo), and LPO·SCN^-·CN^- (buffalo). The difference Fourier $|F_o - F_c|$ maps calculated at this stage revealed interpretable electron densities for glycan chains at four sites with 2 GlcNAc residues and 1 Man at Asn^{95}, 2 GlcNAc residues at Asn^{205}, 2 GlcNAc residues + 1 Man residue at Asn^{241}, and 2 GlcNAc residues at Asn^{332}. The pear-shaped electron densities for SCN^- in both complexes of LPO·SCN^- and an additional linear electron density in the structure of LPO·SCN^-·CN^- were observed in the distal cavity (Figs. 1 and 2). An identical pear-shaped electron density was observed in the structure of LPO·SCN^- (bovine) (supplemental Fig. S1). The electron densities for one calcium ion in each structure were also observed. The difference electron density maps also revealed additional electron densities for seven iodide ions in each structure. All of these were included in the subsequent rounds of refinements. The difference Fourier $\|F_o - F_c\|$ maps at the final stages also indicated excellent additional electron densities for phosphorylation of Ser^{198} in all the three structures. The positions of 339, 398, and 274 water oxygen atoms were determined in the structures of LPO·SCN^- (bovine), LPO·SCN^- (buffalo), and LPO·SCN^-·CN^- (buffalo), respectively. The refinements of the three structures finally converged with R_{work} and R_{free} values of 0.182 (0.236), 0.172 (0.227), and 0.189 (0.238), respectively. The final refinement statistics are included in Table 1. The refined atomic coordinates have been deposited in the Protein Data Bank with codes 3ERI, 3ERH, and 3FAQ, respectively.

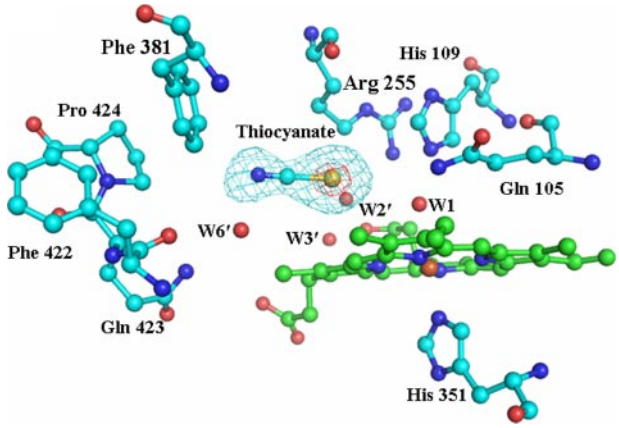

FIGURE 1. **Difference Fourier $|F_o - F_c|$ map indicating the presence of SCN^- ions in the complex of LPO·SCN^-.** The cutoff on the *left* of the pear-shaped electron density corresponds to 2σ (*blue*), and on the *right*, it is at 9σ (*red*).

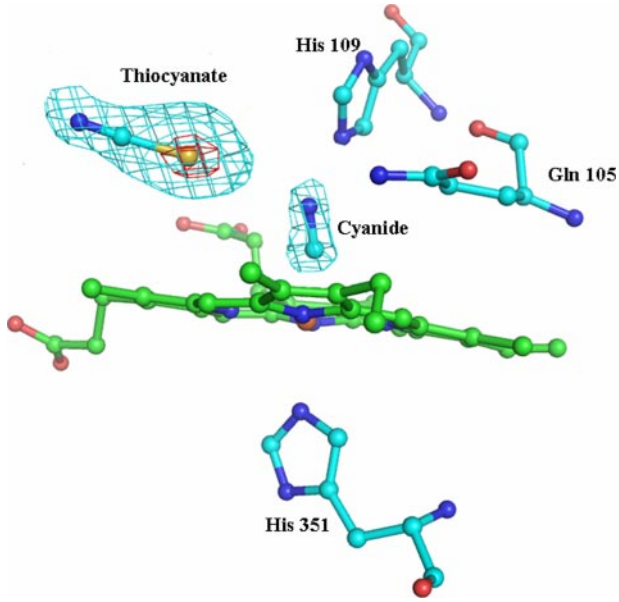

FIGURE 2. **Difference Fourier map calculated in the structures of LPO·SCN^-·CN^- for SCN^- and CN^- ions.** The electron density from the difference Fourier map with 2σ cutoff on the *left* and 9σ cutoff on the *right*. The rod-like density for the CN^- ion is also observed at the distal heme side.

RESULTS

SCN^- Ions in Crystals—The development of color by mixing the filtrates obtained from crystal solution with ferric nitrate confirmed the presence of SCN^- in the crystals. Because the LPO contains a heme group at the active center, the changes in the absorption of heme with regards to ligand binding indicates interactions involving the heme. The spectral studies of (i) LPO·SCN^- crystal solution, (ii) SCN^- ion-free solution, and (iii) protein solutions containing SCN^- were carried out. The heme absorption at 412 nm showed identical values in the shift as well as absorbance with the spectral curves superimposing

TABLE 1

Crystallographic data and refinement statistics

Values in parentheses are for the highest resolution shell. PDB, Protein Data Bank; r.m.s.d., root mean square deviation.

Parameters	Bovine LPO·SCN	Buffalo LPO·SCN	Buffalo LPO·SCN·CN
Crystallographic data			
PDB code	3ERI	3ERH	3FAQ
Space group	$P2_1$	$P2_1$	$P2_1$
Unit cell dimensions	a = 54.5, b = 80.6, c = 77.8 Å; β = 102.6°	a = 54.2, b = 80.5, c = 77.5 Å; β = 102.7°	a = 54.4, b = 80.6, c = 77.8 Å; β = 102.9°
No. of molecules in the unit cell	2	2	2
Estimated solvent content (%)	50	49	49
Resolution range (Å)	70.0–2.5	70.0–2.4	70.0–2.7
Total reflections measured	103,240	101,280	82,220
Unique reflections observed	21,268	25,270	15,890
Redundancy	4.8	4.0	5.2
Completeness (%)	93 (94)	97 (98)	87 (90)
Mosaicity	0.31	0.29	0.87
Overall $I/\sigma(I)$	6.0 (2.0)	6.9 (2.0)	4.5 (2.0)
R_{sym} (%)	8.7 (35.8)	7.9 (28.7)	10.7 (45.5)
Refinement statistics			
Non-H atoms in the model	5304	5378	5256
Protein	4774	4778	4778
Water	339	398	274
SCN^- ions	2	2	2
CN^- ion			1
R_{work} (%)	18.2	17.2	18.9
R_{free} (%)	23.6	22.7	23.8
Mean *B* factors			
Protein atoms (Å^2)	33.9	38.0	43.1
Main chain atoms (Å^2)	33.3	37.3	42.9
Side chain atoms (Å^2)	34.5	38.9	43.4
SCN^- ions (Å^2)	26.0	23.0	37.0
CN^- ions (Å^2)			52.5
Water molecules (Å^2)	38.7	45.4	48.2
r.m.s.d in bond length (Å)	0.02	0.02	0.02
r.m.s.d in bond angle	2.1°	2.0°	2.2°
r.m.s.d in torsion angle	22.1°	20.8°	22.9°
Ramachandran plot statistics (for non-Gly/Pro residues; %)			
Most favored regions	88.1	89.1	85.4
Additionally allowed regions	10.4	9.5	13.2
Generously allowed regions	1.5	1.4	1.4

well for the samples of crystal and protein solution with SCN^- ions. However, the measurements carried out on the SCN^- ion-free samples showed different values, and the absorption curve did not superimpose on spectral curves obtained for the sample containing SCN^- ions. These experiments clearly indicated that the SCN^- ions are present in the crystals of the LPO enzyme.

Overall Protein Structure—The crystallographic parameters and refinement statistics for the crystal structure of the complex of lactoperoxidase with thiocyanate (LPO·SCN^-) are given in Table 1. The structure determination clearly revealed that a thiocyanate ion is present in the distal heme cavity with the sulfur atom of the SCN^- ion being nearer to the heme iron atom than its nitrogen atom. The overall structural organization of the complex of LPO·SCN^- is shown in Fig. 3. One of the most remarkable features of the structure of the LPO·SCN^- complex is the placement of the SCN^- ion, which is supported by favorable conformation of the loop Arg^{418}–Phe^{431}. The structure of the corresponding loop is strikingly different in MPO (Fig. 4). This loop constitutes one of the walls of the substrate-binding site. The structure of this rigid loop is stabilized by a salt bridge between His^{426} and Glu^{130} from helix H_2a. The helix H_2a is a unique feature of LPO. The iron atom is displaced approximately by 0.1 Å toward proximal His^{351} from the plane made by four heme nitrogen atoms. The four pyrrole rings of the heme group are planar, whereas the heme group as a whole

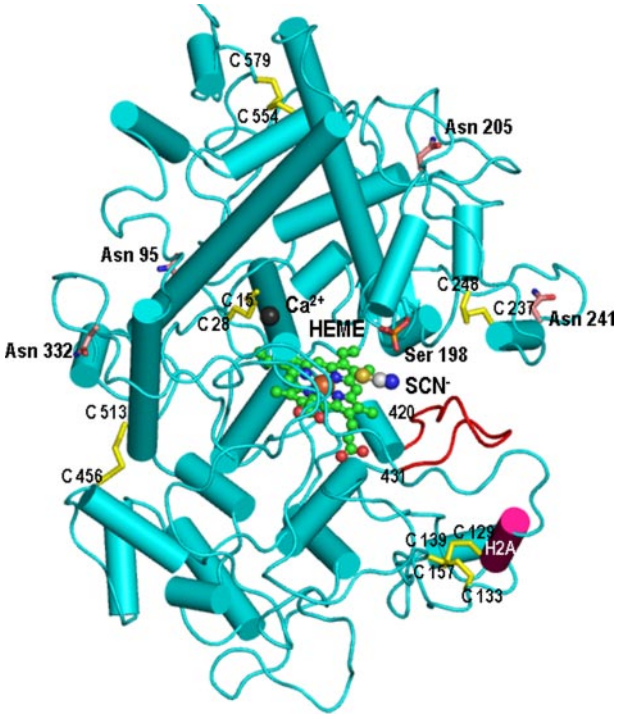

FIGURE 3. **Structure of LPO·SCN^- complex.** The heme group (*green*), the SCN^- ion, and Ca^{2+} (*black*) are also shown. The loop Arg^{418}–Phe^{431} is indicated in *red*. Helix H_2a is shown in *purple*, whereas disulfide bonds are presented in *yellow*.

is slightly non-planar. The bond angles at the iron atom, 208 N1A-Fe-N1C and 208 N1B-Fe-N1D, are 165.8° and 166.2°, respectively, indicating that heme iron atom is equally of the lines of N1A-N1C and N1B-N1D.

Binding of SCN^-—The LPO enzyme catalyzes the peroxidation of thiocyanate in the presence of H_2O_2. In order for the reaction to occur, the SCN^- ion must bind to LPO at the substrate-binding site in the distal heme cavity with a favorable orientation. The most important question arises here as to how the stereochemical environment around the heme moiety in LPO determines the preference for the SCN^- ion so as to make it a preferred substrate. The structure determination has shown an excellent pear-shaped electron density at the distal site, indicating optimum conditions for binding. The observed density at one end corresponds to nearly 9σ, whereas at the other end, it is equivalent to the 2σ cutoff (Fig. 1). The heme environment in the native LPO is characterized by a unique water structure at the distal heme cavity. The binding of different ligands occurs by displacing appropriate water molecules for the ligands to act either as a substrate or as an inhibitor. The positions of conserved water molecules Wat^1, $Wat^{2'}$, $Wat^{3'}$, $Wat^{4'}$, $Wat^{5'}$, and $Wat^{6'}$ (Fig. 5*a*) occupy the space in the distal site in the proximity of heme moiety, whereas an array of another set of conserved water molecules Wat^1, Wat^2, Wat^3, Wat^4, Wat^5, and Wat^6 presumably facilitates catalytic activity by relaying the proton from H_2O_2 to the surface of the protein. Recently, compelling experimental evidence has shown

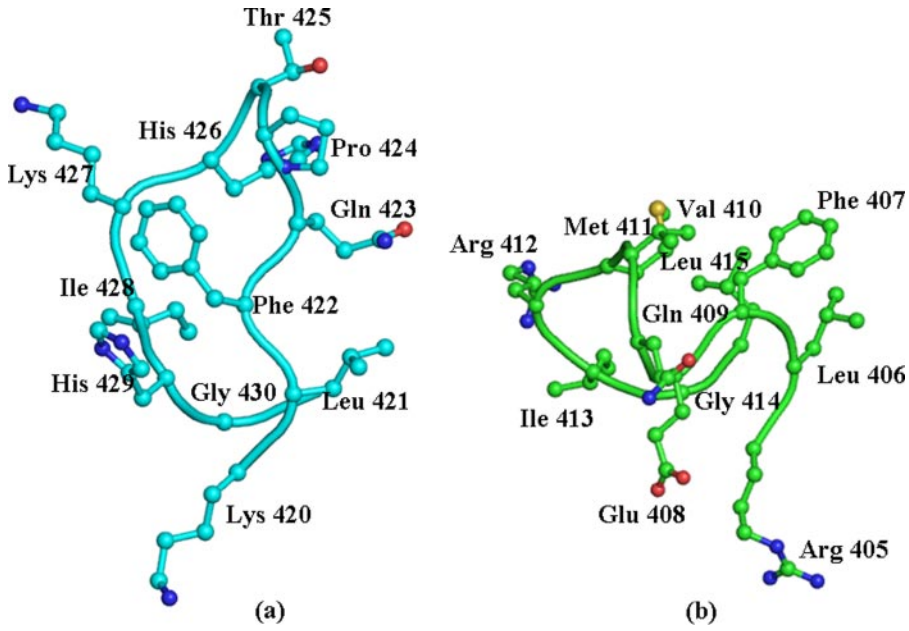

FIGURE 4. **The conformation of the loop that forms one of the walls of the substrate binding channel and determines the shape of the substrate-binding site in LPO (*a*) MPO (*b*).** Gln^{423} in LPO and Phe^{407} in MPO are particularly important for inducing the orientations of the SCN^- ion in the distal cavity.

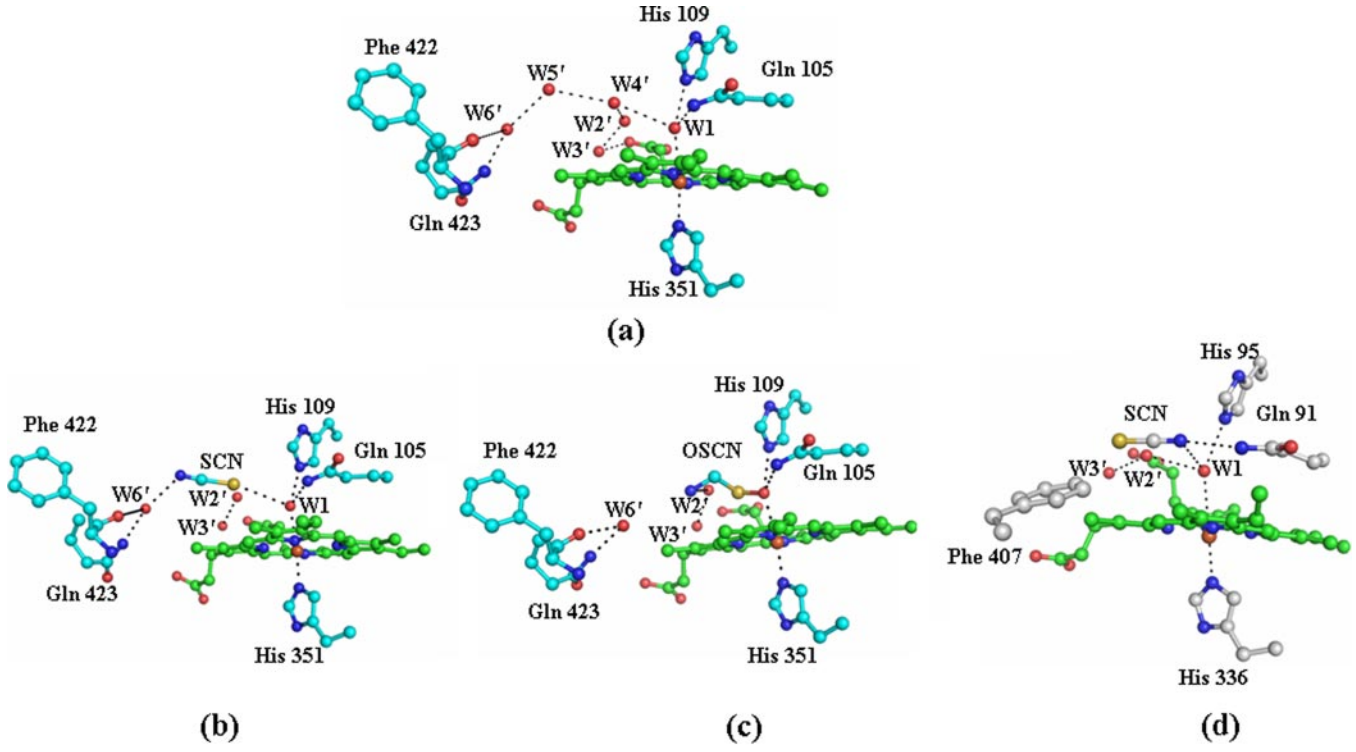

FIGURE 5. The conserved water molecules in the proximity of the heme moiety of the native enzyme, Wat^1, $Wat^{2'}$, $Wat^{3'}$, $Wat^{4'}$, $Wat^{5'}$, and $Wat^{6'}$, are illustrated (*a*). The binding of thiocyanate/hypothiocyanate ions is also shown in the distal heme cavity. The orientations of the SCN^- ion in the LPO·SCN^- complex (*b*), the $OSCN^-$ ion in the LPO·$OSCN^-$ complex (*c*), and SCN^- ion in the MPO·SCN^- complex (*d*) are shown. *W*, water.

that such an array of water molecules may function as a proton transfer chain (28–31). It is expected that ligand binding in the distal site either displaces or deletes one or more conserved water molecules. In the present complex, the binding of thiocyanate in the distal site results in the deletion of two water molecules, $Wat^{4'}$ and $Wat^{5'}$, whereas $Wat^{2'}$ and $Wat^{3'}$ are shifted away considerably. The observed orientation of the SCN^- ion in the distal site shows that the sulfur atom is placed toward the heme iron at a distance of 3.2 Å from Wat^1 and 4.2 Å from His^{109} $N^{\epsilon 2}$, whereas the nitrogen atom is located away from Wat^1 and forms a hydrogen bond with Gln^{423} $N^{\epsilon 2}$ through a conserved, well stabilized water molecule, $Wat^{6'}$ (Fig. 5*b*). In addition to interactions with Gln^{423} $N^{\epsilon 2}$ and the nitrogen atom of SCN^-, $Wat^{6'}$ is also hydrogen-bonded to Phe^{422} oxygen. In another recent structure of the lactoperoxidase complex with its product $OSCN^-$ (LPO·$OSCN^-$), the orientation of the $OSCN^-$ ion was also found similar to that of the SCN^- ion, as observed in the present LPO·SCN^- complex where the sulfur atom is closer to heme iron than the nitrogen atom (Fig. 5*c*) (32). A similar orientation of the SCN^- ion has also been reported in the structure of octaheme tetrathionate reductase (33). An identical arrangement for the SCN^- ion in the distal cavity was also observed in the structure of the complex of LPO·SCN^- (bovine) (supplemental Fig. S2). The superimposition of distal heme cavities of LPO·SCN^- (buffalo) and LPO·SCN^- (bovine) shows a root mean square shift of 0.05 Å for 124 atoms (supplemental Fig. S3). These results are in striking contrast to the observation made in the MPO·SCN^- complex where the nitrogen atom was reported to be closer to the heme iron, whereas the sulfur atom was placed farther away (Fig. 5*d*). It also should be mentioned that NMR relaxation methods (34–36) indicate that in the LPO·SCN^- complex, the nitrogen atom is closer to the heme iron than the carbon. However, the reported distances in the two studies were unusually different for drawing a definite conclusion. It is also noteworthy here that the plane of the SCN^- ion is almost parallel to the heme plane in the LPO·SCN^- complex with a 9.5° angle between the plane of the heme and the SCN^- ion. It is pertinent to note that the substrate-binding pocket in the distal heme cavity is surrounded by the heme moiety on one side, whereas the side chain of Arg^{255} with C^β and C^γ atoms forms the opposite hydrophobic side. The third side consists of a conserved water molecule ($Wat^{6'}$), Gln^{423}, Phe^{422} oxygen, Pro^{424}, and Phe^{381}, and the fourth side is made by Gln^{105} and His^{109} with other conserved water molecules of the distal site, including Wat^1. The observed position of the SCN^- ion is delicately balanced by van der Waals forces from the nearest heme moiety atoms on one side and C^β and C^γ atoms of Arg^{255} on the other. The plane of heme moiety is nearly planar, and it is nearly parallel to the C^β–C^γ bond of Arg^{255}. The conserved water molecule stabilized by interactions with Gln^{423} $N^{\epsilon 2}$, and Phe^{422} oxygen locks the position of the nitrogen atom of the SCN^- ion. This is also supported by the side chains of Pro^{424} and Phe^{381}. This shows that the stereochemistry in LPO appears to be specific for the binding of the SCN^- ion in the distal heme cavity. In contrast, a similar environment is not available in MPO. The most notable structural element in LPO seems to be the conformation of the Arg^{418}–Phe^{431} loop in LPO, which is strikingly different from that of the corresponding loop in MPO. This loop in MPO adopts a conformation that places Phe^{407} at the site occupied by the side chain of Gln^{423} and the conserved water molecule $Wat^{6'}$. Therefore, the orientation of the SCN^- ion in MPO is bound to differ from that of LPO. This seems to have evolved to attain substrate specificity in mammalian peroxidases. It is also noteworthy that the SCN^- plane is inclined at a much larger angle (70.4° in molecule A and 35.2° in molecule B in the structure of the MPO dimer) in the MPO·SCN^- complex (37). The fact that the SCN^- ion is inclined at different angles in the two molecules of the MPO dimer is itself an indication of low grade binding specificity for the SCN^- ion in MPO. The corresponding angle between the planes of $OSCN^-$ and the heme moiety in the complex of LPO·$OSCN^-$ was reported to be 21.5° (32). The plane of the SCN^- ion in the LPO·SCN^- complex is shifted away from the line of His^{351}-Fe-His^{109} by ~3.8 Å, whereas in the complex of MPO·SCN^-, it is at a distance of 3.3 Å.

Comparison with the Structure of LPO·SCN^-·CN^-—The crystals of LPO·SCN^- were soaked in the mother liquor containing 100 mM NaCN. The presence of CN^- in the crystals was verified by spectroscopic and chemical methods.[5] The x-ray intensity data on the crystals of LPO·SCN^-·CN^- were collected to 2.7 Å resolution, and the structure was refined to R_{work} and R_{free} factors of 0.189 and 0.238, respectively (Protein Data Bank Code 3FAQ). The major features of the difference Fourier maps were examined in the vicinity of heme moiety. An elongated positive peak at the 3.0σ cutoff on the distal side of the heme iron at the position of the conserved water molecule Wat^1 was interpreted as cyanide binding to the heme iron (Fig. 2). It also showed a pear-shaped electron density for the SCN^- ion (Fig. 2). The refined structure shows a heme iron-to-cyanide carbon distance of 1.9 Å. It is considerably shorter than the distance of the heme iron to the water oxygen atom of 2.6 Å in the LPO·SCN^- complex. The C–N bond in the cyanide ion is almost perpendicular to the heme plane with a Fe–C–N bond angle of 161.0°. The position of the SCN^- ion in the present structure is identical to that observed in the structure of LPO·SCN^-. However, the plane of the SCN^- ion is not as parallel (inclination, 51°) as that found in the complex of LPO·SCN^- (inclination, 10°), indicating a slight adjustment upon binding of the cyanide ion. This is in striking contrast to the binding of the SCN^- ion in MPO, where the planes of the heme moiety and SCN^- ion are considerably more inclined in the MPO·SCN^- complex (Protein Data Bank Code 1DNU) (inclination, 70°) than in the ternary complex of MPO·SCN^--CN^- (inclination, 15°) (Protein Data Bank Code 1DNW). The orientations of the SCN^- ion, with the sulfur atom of SCN^- being closer to the heme iron than its nitrogen atom in both structures of LPO·SCN^- and LPO·SCN^-·CN^-, are found to be identical. It may also be mentioned here that the $OSCN^-$ in the complex of LPO·$OSCN^-$ (32) has a similar orientation as in the present structure.

[5] I. A. Sheikh, A. K. Singh, N. Singh, M. Sinha, S. B. Singh, A. Bhushan, P. Kaur, A. Srinivasan, S. Sharma, and T. P. Singh, unpublished data.

DISCUSSION

Thiocyanate is a primary physiological substrate for lactoperoxidase. The substrate-binding channel in mammalian peroxidases is extended from the distal heme cavity to the surface of the protein. In LPO, this channel consists of loop Arg^{418}–Phe^{431} on one side, whereas loops Ser^{190}–Gly^{194}, Lys^{232}–Thr^{243}, Ala^{251}–Ala^{256}, and Glu^{373}–Asn^{382} make the opposite side. The conformation of the loop Arg^{418}–Phe^{431} (Fig. 4*a*) is strikingly different from that of the corresponding loop Arg^{403}–Leu^{415} in MPO (Fig. 4*b*). As a result, the shapes of the substrate-binding sites as well as the chemical environments are considerably different in LPO and MPO molecules. In LPO, the inner sides of the channel walls contain predominantly hydrophobic and positively charged residues such as Lys^{233}, Phe^{239}, His^{377}, Phe^{380}, Phe^{381}, Phe^{422}, Gln^{423}, Lys^{427}, and His^{429}. The corresponding residues in MPO are Leu^{216}, Leu^{223}, Ser^{362}, Phe^{365}, Phe^{366}, Phe^{407}, Glu^{408}, Arg^{412}, and a deletion at the position corresponding to His^{429} in LPO. It also indicates a stronger positive charge environment in LPO. The back of the channel is made by the heme moiety, which is sandwiched between two antiparallel helices H2 (98–111) and H8 (341–353). The SCN^- ion is placed almost parallel to the plane of the heme moiety with the sulfur atom being closer to the heme iron than its nitrogen atom. The Fe-S distance is 4.9 Å, and the Fe-N distance is 7.4 Å. The opposite has been reported in the complex of MPO·SCN^- where the Fe-S distance is 6.2 Å and the Fe-N distance is 4.9 Å. The plane of the SCN^- ion in the LPO·SCN^- complex is only inclined at 11.0°, whereas in MPO the observed inclination is of the order of 70°. The placements of the SCN^- ion in the structures of LPO and MPO are supported by the stereochemical environments of their heme moieties. In the observed orientation of the SCN^- ion in LPO, the sulfur atom is hydrogen-bonded to the conserved water molecule Wat^1, whereas Wat^1 is, as usual, linked to the heme iron at a distance of 2.6 Å and hydrogen-bonded to His^{109} $N^{\epsilon 2}$ at a distance of 2.5 Å. The nitrogen atom of the SCN^- ion is hydrogen-bonded to another conserved water molecule, $Wat^{6'}$, which in turn is hydrogen-bonded to Gln^{423} $N^{\epsilon 2}$ and Phe^{422} oxygen. Gln^{423} $N^{\epsilon 1}$ is linked to two other water molecules. These water molecules interact with Glu^{116} and the carboxylate of the ring D heme propionate. This network is further stabilized by the participation of Arg^{440} and Phe^{161}. In contrast, the position of Gln^{423} in LPO is occupied by Phe^{407} in MPO, whereas the conserved water molecule $Wat^{6'}$ is absent in MPO. Actually, the real turning point in the structure of loop Arg^{418}–Phe^{431} occurs at Phe^{422} in LPO and Phe^{407} in MPO. Both Phe^{422} in LPO and the corresponding Phe^{407} in MPO turn in opposite directions. The observed conformation of Phe^{422} in LPO is induced by a type III β-turn formed for tetrapeptide Gln^{423}-Pro^{424}-Thr^{425}-His^{426}, which is stabilized by an intra turn hydrogen bond involving Gln^{423} oxygen and His^{426} nitrogen. In addition, this tight turn is stabilized by interactions of Gln^{423} with the solvent-rich polar environment, sterically favorable Pro residue, and a salt bridge involving His^{426} with Glu^{130}. As a result, Phe^{422} adopts a conformation with ϕ and ψ torsion angles of −105.8° and 126.0°, respectively, making the side chain of Phe^{422} a part of a hydrophobic cluster formed by Phe^{380}, Phe^{381}, Pro^{236}, Phe^{239}, and Pro^{234}. In contrast, the values of ϕ and ψ torsion angles of Phe^{407} in MPO are 58.1° and 28.3°, respectively, as a result of which the side chain of Phe^{407} moves to occupy the position of Gln^{423} and conserved water molecule $Wat^{6'}$. It may also be mentioned that the conformation of loop Arg^{403}–Leu^{415} in MPO is internally rigidified by the presence of three tight β-turns for three overlapping tetrapeptides, Arg^{405}-Leu^{406}-Phe^{407}-Glu^{408} (type II β-turn), Phe^{407}-Glu^{408}-Gln^{409}-Val^{410} (type III β-turn), and Glu^{408}-Gln^{409}-Val^{410}-Met^{411} (distorted type III β-turn). This is a peculiar conformation with a high degree of rigidity in MPO. It is pertinent to note here that the conformation of the loop in LPO is also considerably influenced by the presence of an extra residue, His^{429}. (The corresponding residue is absent in MPO, which interacts with Phe^{380} oxygen through a water molecule, Wat^{118}. The corresponding interaction does not exist in MPO.) Additionally, His^{426} is hydrogen-bonded to Glu^{130} from the neighboring helical segment in LPO. The corresponding segment is formed very differently in MPO due to the absence of a hexapeptide Ser^{121} to Lys^{126} (LPO numbering) in the sequence of MPO. As a result, a similar interaction is absent in MPO. Overall, the loop Arg^{418}–Phe^{431} is involved in a larger number of inter-loop interactions in LPO than in MPO. On the other hand, intra-loop interactions are stronger in MPO than in LPO. Therefore, the stereochemical environment in the proximity of the heme moiety in LPO is indeed considerably different from that of MPO. The effect of this local structure in the proximity of the heme moiety in LPO may guide the placement differently of its substrate SCN^- ion, resulting in the orientation that is unique and appropriate for the catalytic action by the enzyme. As far as the positioning of the SCN^- ion in MPO is concerned, its placement with the sulfur atom being away appears to be less favorable for catalytic action, thus making it a poor substrate for the enzyme MPO. Even so, the structural arrangements in MPO in the resting state may not be able to induce a favorable orientation of the SCN^- ion; the workable orientation may occur in the presence of H_2O_2 when compound I is formed. Nevertheless, an appropriate orientation of SCN^- that is induced by protein structure will make the mechanism of action highly efficient. This is reflected in terms of the turnover rates reported for enzymes LPO and MPO with the substrate SCN^-, which is more than 20 times higher for LPO than that of MPO (38). To confirm the reproducibility of the orientation of the SCN^- ion in the distal site, we have determined other crystal structures of LPO with the SCN^- ion under different conditions (Protein Data Bank code 3ERI), and indeed, we repeatedly observed the orientations of the SCN^- ion that are identical to the orientation being reported here in the LPO·SCN^- complex. Therefore, this orientation of the SCN^- ion is specific to LPO and is the correct orientation for efficient enzymatic catalysis by LPO. However, it does not rule out the conversion of SCN^- to $OSCN^-$ by other mammalian peroxidases because the converted form after the reaction of the resting enzyme with H_2O_2 to compound I may induce the required orientation for catalysis.

It has been shown that the preincubation of the SCN^- ion with mammalian peroxidases LPO, MPO and eosinophil peroxidase alters the rates of their catalytic activities (39). The

bound SCN^- ion at the distal site may restrict the accessibility of the binding site to H_2O_2. Additionally, the SCN^- ion interacts with heme water molecule Wat^1, thus enhancing the binding affinity of water. As a result, it would be more difficult for H_2O_2 to displace Wat^1. The above two factors will have adverse effects for the affinity of H_2O_2, resulting in reducing the rate of reaction. However, the stereochemical characteristics of the substrate-binding site in the resting LPO allow SCN^- to bind with favorable orientation in LPO, whereas in MPO, SCN^- is held with unfavorable orientation. Therefore, this will also adversely affect the efficiency of the catalytic function of MPO for the substrate SCN^-. In summary, the results of these investigations clearly establish the structural preference of the SCN^- ion as a good substrate for LPO and mediocre substrate for MPO.

REFERENCES

1. Nichol, A. W., Angel, L., A., Moon, T., and Clezy, P. S. (1987) *Biochem. J.* **247,** 147–150
2. Ciaccio, C., Sanctis, G. D., Marini, S., Sinibaidi, F., Santucci, R., Arcovito, A., Bellelli, A., Ghibaudi, E., Rosa, F. P., and Coletta, M. (2004) *Biophys. J.* **86,** 448–454
3. Thomson, R., Jensen, L. S., Gleich, G. J., and Claus, O. (2000) *Arch. Biochem. Biophys.* **379,** 147–152
4. Tanaka, T., Sato, S., Kumura, H., and Shimazaki, K. (2003) *Biosci. Biotechnol. Biochem.* **67,** 2254–2261
5. DePillis, G. D., Ozaki, S., Kuo, J, M., Malthy, D. A., and Ortiz de Montellano, P. R. (1997) *J. Biol. Chem.* **272,** 8857–8860
6. Klebanoff, S. (1970) *Science* **169,** 1095–1097
7. Klebanoff, S. (1999) *Proc. Assoc. Am Phys.* **111,** 383–389
8. Wang, J., and Slungaard, A. (2006) *Arch. Biochem. Biophys.* **445,** 256–260
9. Ruf, J., and Carayon, P. (2006) *Arch. Biochem. Biophys.* **445,** 269–277
10. Fenna, R., Zeng, J., and Davey, C. (1995) *Arch. Biochem. Biophys.* **316,** 653–656
11. Taylor, L. K., Pohl, J., and Kinkade, J. M. (1992) *J. Biol. Chem.* **267,** 25282–25288
12. Fiedler, T. J., Davey, C. A., and Fenna, R. E. (2000) *J. Biol. Chem.* **275,** 11964–11971
13. Singh, A. K., Singh, N., Sharma, S., Singh, S. B., Kaur, P., Bhushan, A., Srinivasan, A., and Singh, T. P. (2008) *J. Mol. Biol.* **376,** 1060–1075
14. Kooter, I. M., Moguilevsky, N., Bollen, A., Sijtsema, N. M., Otto, C., and Wever, R. (1997) *J. Biol. Inorg. Chem.* **2,** 191–197
15. Oram, J. D., and Reiter, B. (1996) *Biochem. J.* **100,** 382–388
16. Hoogendoorn, H., Piessens, J. P., Scholtes, W., and Stodard, L. A. (1977) *Caries Res.* **11,** 77–84
17. Zgliczynski, J. M., Selvaraj, R. J., Paul, B. B., Stelmaszynska, T., Poskitt, P. K., and Sbarra, A. J. (1977) *Proc. Soc. Exp. Biol. Med.* **154,** 418–422
18. Bakkenist, A. R., de Boer, J. E., Plat, H., and Wever, R. (1980) *Biochim. Biophys. Acta* **613,** 337–348
19. Wolfson, L. M., and Sumner, S. S. (1993) *J. Food Prot.* **56,** 887–892
20. Shindler, J. S., and Bardsley, W. G. (1975) *Biochem. Biophys. Res. Commun.* **67,** 1307–1312
21. Goldstein, F. (1950) *J. Biol. Chem.* **187,** 523–527
22. Otwinowski, Z., and Minor, W. (1997) *Methods Enzymol.* **276,** 307–326
23. McCoy, A. J., Grosse-Kunstleve, R. W., Storoni, L. C., and Read, R. J. (2005) *Acta Crystallogr. Sect. D* **61,** 458–464
24. Murshudov, G. N., and Dodson, E. J. (1997) *Protein Crystallogr.* **33,** 31–38
25. Collaborative Computational Project No. 4 (1994) *Acta Crystallogr. Sect. D* **50,** 760–763
26. Jones, T. A., Zou, J., Cowan, S. W., and Kjeldgard, M. (1991) *Acta Crystallogr. Sect. A* **47**, 110–118
27. Emsley, P., and Cowtan, K. (2004) *Acta Crystallogr. Sect. D* **60,** 2126–2132
28. Geissler, P. L., Dellago, C., Chandler, D., Hutter, J., and Parrinello, M. (2001) *Science* **291,** 2121–2124
29. Mohammed, O. F., Pines, D., Dreyer, J., Pines, E., and Nibbering, E. T. J. (2005) *Science* **310,** 83–86
30. Ando, K., and Hynes, J. T. (1997) *J. Phys. Chem.* **101,** 10464–10478
31. Ando, K. (1999) *J. Phys. Chem.* **103,** 10398–10408
32. Singh, A. K., Singh, N., Sharma, S., Shin, K., Takase, M., Kaur, P., Srinivasan, A., and Singh, T. P. (2009) *Biophys. J.* **96,** 646–654
33. Mowat, C. G., Rothery, E., Miles, C. S., McIver, L., Doherty, M. K., Drewette, K., Taylor, P., Walkinshaw, M. D., Chapman, S. K., and Reid, G. A. (2004) *Nat. Struct. Mol. Biol.* **11,** 1023–1024
34. Modi, S., Behere, D. V., and Mitra, S. (1989) *Biochemistry* **28,** 4689–4694
35. Modi, S., Behere, D. V., and Mitra, S. (1990) *Indian J. Chem.* **29A,** 301–311
36. Crull, G. B., and Goff, H. M. (1993) *J. Inorg. Biochem.* **15,** 181–192
37. Blair-Johnson, M., Fiedler, T., and Fenna, R. (2001) *Biochemistry* **40,** 13990–13997
38. Furtmuller, P. G., Jantschko, W., Zederbauer, M., Jakopitsch, C., Arnhold, J., and Obinger, C. (2004) *Jpn. J. Infect. Dis.* **57,** S30–S31
39. Tahboub, Y. R., Galijasevic, S., Diamond, M. P., and Abu-Soud, H. M. (2005) *J. Biol. Chem.* **280,** 26129–26136